

# Experimental Observation of a Topological Phase in the Maximally Entangled State of a Pair of Qubits

Jiangfeng Du<sup>1,2,\*</sup>, Jing Zhu<sup>1</sup>, Mingjun Shi<sup>1</sup>, Xinhua Peng<sup>2</sup>, and Dieter Suter<sup>2</sup>

<sup>1</sup> Hefei National Laboratory for Physical Sciences at Microscale and Department of Modern Physics, University of Science and Technology of China, Hefei, Anhui 230026, People's Republic of China

<sup>2</sup>Fachbereich Physik, Universität Dortmund, 44221 Dortmund, Germany

(Dated: November 2, 2018)

Quantum mechanical phase factors can be related to dynamical effects or to the geometrical properties of a trajectory in a given space - either parameter space or Hilbert space. Here, we experimentally investigate a quantum mechanical phase factor that reflects the topology of the SO(3) group: since rotations by  $\pi$  around antiparallel axes are identical, this space is doubly connected. Using pairs of nuclear spins in a maximally entangled state, we subject one of the spins to a cyclic evolution. If the corresponding trajectory in SO(3) can be smoothly deformed to a point, the quantum state at the end of the trajectory is identical to the initial state. For all other trajectories the quantum state changes sign.

PACS numbers: 03.65.Vf, 03.67.Mn, 76.60.-k

Quantum phase factors are ubiquitous and have been crucial in explaining many phenomena that appear to be unrelated. The overall phase change resulting from the  $2\pi$  rotation of a particle, e.g., distinguishes Fermions from Bosons or categorizes Anyons [1]. If more general circuits are considered than simple  $2\pi$  rotations, the states can acquire arbitrary phases even for Fermions and Bosons [2, 3, 4]. These phases can be split into two parts, which are referred to as dynamic and geometric. The dynamic phase is related to the energy expectation value of the quantum state, integrated over the trajectory, while the geometric part is related only to the geometry of the circuit. This analysis of quantum phases in terms of dynamical and geometrical phases was used extensively over the past decades to discuss a wide range of quantum phenomena [5].

This picture appears to be not quite complete, however, if we consider the evolution of pairs of spins  $1/2$  in a maximally entangled state (MES). If one of the two spins undergoes a rotation (i.e. a local transformation), the system acquires neither a dynamical nor a geometrical phase [6], except at some points, where it abruptly changes by  $\pi$  [7]. It may thus be more appropriate to relate this *sudden* phase change to the topology of the appropriate space, i.e. to its connectedness, rather than to the geometry, i.e. its curvature [7].

If we consider rotations of single qubits, the appropriate space is that of the rotations in  $R^3$ , which form a representation of SO(3). Its elements can be considered to form a sphere, where the direction of each point corresponds to the rotation axis and the distance from the origin to the rotation angle. Since rotations by  $\pi$  around opposite directions are indistinguishable in  $R^3$  and corresponding elements of SO(3) are identical, opposite points on the surface of the SO(3) sphere have

to be identified. A trajectory that crosses the surface of the sphere immediately re-enters it at the opposite point. A trajectory that penetrates the surface once cannot be smoothly deformed into one that does not cross the surface. Closed trajectories can thus be classified into “+” and “-” classes, depending on the number of times they cross the surface.

This behavior can be directly mapped into the phases of the quantum states of maximally entangled spin pairs, where one of the two spins is rotated around a (possibly time-dependent) magnetic field. For an arbitrary *cyclic* sequence  $C$  of rotations of the single qubit, i.e. arbitrary trajectories in SO(3), the MES is transformed into

$$|\Psi\rangle_{MES}(C) = (-1)^n |\Psi\rangle_{MES}(0)$$

where  $|\Psi\rangle_{MES}(0)$  is the initial state and  $n$  is the number of times the trajectory penetrates the surface of the SO(3) sphere. Milman and Mosseri therefore call this phase a topological phase, since it appears to be related to the double-connectedness of SO(3) [7].

While Milman and Mosseri considered trajectories consisting of discrete rotations around fixed axes, LiMing et al [8] found the same behavior for trajectories where the rotation axis changes continuously. They also discussed the possibility of observing the phase in an optical interference experiment.

In this paper, we report an experimental verification of this topological phase by NMR interferometry. For this purpose, we initialize a system of two nuclear spins into a (pseudo-)maximally entangled state and apply radio-frequency pulses that rotate one of the two spins through trajectories that correspond either to the “+” or “-” type. In the first case, the resulting signal is identical to that of the reference system, which is not rotated, in the second case, we observe a phase change by  $\pi$ .

The topology of SO(3) can, in principle, be explored by letting single qubits undergo the corresponding rotations. However, in this case, the resulting phase factors contain dynamical as well as geometrical contributions [9, 10]. In

---

\*Electronic address: djf@ustc.edu.cn

the present context, Maximally Entangled States (MES) of two qubits offer a useful alternative. If we initially prepare the system in a MES and apply local transformations (i.e. rotations) to one of the two qubits, the system always remains in an MES and does not acquire any dynamical phase.

A general two-qubit MES can be written as

$$|\Psi\rangle = \sqrt{\frac{1}{2}}(\alpha|00\rangle + \beta|01\rangle - \beta^*|10\rangle + \alpha^*|11\rangle), \quad (1)$$

where the coefficients  $\alpha$  and  $\beta$  are normalized to unity:  $\alpha\alpha^* + \beta\beta^* = 1$ . Without loss of generality, we choose to initialize the system in the Bell state

$$|\Psi\rangle_{MES}(0) = \sqrt{\frac{1}{2}}(|00\rangle + |11\rangle) \quad (2)$$

(i.e.  $\alpha = 1, \beta = 0$ ), and apply the rotations to the first of the two qubits. At every point in time, we can thus identify the state of the system

$$|\Psi\rangle_{MES}(t) = (U_{\hat{n}}(\theta) \otimes \mathbf{1}) |\Psi\rangle_{MES}(0) \quad (3)$$

with the corresponding element of SO(3). Here,  $U_{\hat{n}}$  describes the unitary transformation implementing the trajectory on the first qubit and  $\mathbf{1}$  is the unit operator acting on the second qubit of the MES. The unit vector  $\hat{n}$  defines the overall rotation axis and  $\theta$  the rotation angle, which corresponds in SO(3) to the distance from the origin.

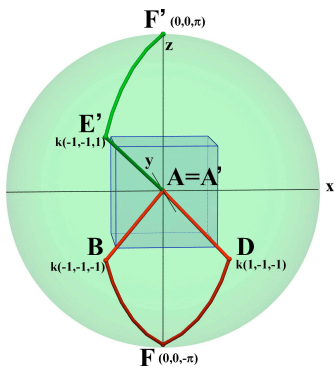


FIG. 1: (Color online) We consider two different trajectories in SO(3). The red curve  $A \rightarrow B \rightarrow F \rightarrow D \rightarrow A$  belongs to the “+” class, since it does not cross the surface of the sphere. The trajectory  $A \rightarrow B \rightarrow F = F' \rightarrow E' \rightarrow A'$  belongs to the “-” class. Only the second part differs from the first trajectory; it is drawn in green.  $k = \frac{2\pi}{3\sqrt{3}} \approx 1.21$ .

We consider the two types of trajectories shown in Fig. 1. [6] In each case, the first two rotations take the system from the origin (point A in Fig. 1) to point B and from there to point F. The trajectories are chosen such that F corresponds to a rotation by  $\pi$ ; it is therefore located on the surface of the SO(3) sphere and is equivalent to point F' at the opposite position. From here, the “+” trajectory returns to the origin via point D, i.e. without crossing the boundary, but the “-” trajectory returns

via E'. Since it “jumps” from F to F', the associated quantum state changes sign.

Each of the segments of the trajectories represented in Fig. 1 correspond to a rotation by  $\theta = \frac{2\pi}{3}$  around one of the cube diagonals axes. Table I lists the rotation axes for each segment of both trajectories.

TABLE I: Rotation axes of all segments of the “+” and “-” trajectories.

“+” class $ABFDA$	“-” class $ABF'E'A'$
$AB : \sqrt{1/3}(-1, -1, -1)$	$AB : \sqrt{1/3}(-1, -1, -1)$
$BF : \sqrt{1/3}(1, -1, -1)$	$BF : \sqrt{1/3}(1, -1, -1)$
$FD : \sqrt{1/3}(-1, -1, 1)$	$F'E' : \sqrt{1/3}(1, -1, -1)$
$DA : \sqrt{1/3}(-1, 1, 1)$	$E'A' : \sqrt{1/3}(1, 1, -1)$

The difference between the two circuits is an overall phase factor acquired by the quantum state. Since this does not affect directly observable quantities of the system, one usually resorts to interferometric experiments for observing the sign change. Milman and Mosseri [7] suggested using optical interferometry for this purpose. Here, we resort to NMR interferometry [9].

For this purpose, we have to introduce an ancilla qubit that is coupled to the two qubits forming the MES. As shown in Fig. 2, the ancilla qubit is initialized into an equal superposition by applying a Hadamard gate to the  $|0\rangle$  state. This Hadamard gate corresponds to the first beam splitter in a Mach-Zehnder interferometer. After this gate, the system is in the state

$$|\psi(0)\rangle = \frac{1}{\sqrt{2}}(|0\rangle + |1\rangle) \otimes |\Psi\rangle_{MES}. \quad (4)$$

Here, the first qubit is the ancilla qubit and qubits 2 and 3 form the MES.

Instead of the simple unitary operation corresponding to the trajectories in SO(3), we then use conditional rotations, which only act on that “copy” of the MES that is connected to the  $|1\rangle$  state. After this controlled cyclic circuit, the system reaches the state

$$|\psi(cU_{\pm})\rangle = \frac{1}{\sqrt{2}}(|0\rangle \pm |1\rangle) \otimes |\Psi\rangle_{MES}, \quad (5)$$

where the  $\pm$  signs refer to the corresponding circuit class. If we trace over the qubits 2 and 3, we apparently obtain the sign information by measuring the expectation value of

$$\langle \sigma_x^1 \rangle = \pm 1,$$

where the sign again relates to the circuit class.

As a quantum register for these experiments, we selected the three  $^{19}\text{F}$  nuclear spins of Iodotrifluoroethylene ( $\text{F}_2\text{C}=\text{CFI}$ ). This system has relatively strong couplings between the nuclear spins, large chemical shifts, and long decoherence times. The experiments were performed on a Bruker Avance II 500 MHz (11.7 Tesla) spectrometer equipped with a QXI probe with pulsed field

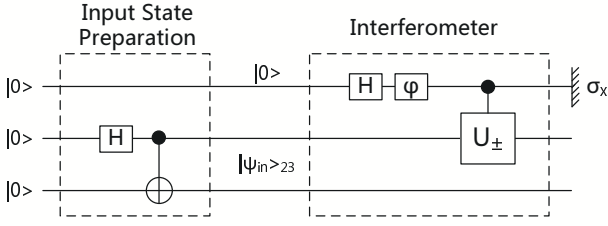


FIG. 2: Quantum network representation of input state preparation and interferometric measurement. The initial state is  $|000\rangle$ . H is a pseudo-Hadamard gate  $H = e^{-i\frac{\pi}{2}I_y}$  rotating the qubit by the angle  $\frac{\pi}{2}$  about the Y axis, gate  $\varphi = e^{-i\varphi I_z}$  rotating the qubit by the angle  $\varphi$  about the Z axis.

gradient. The resonance frequency for the  $^{19}\text{F}$  spins is around 470.69 MHz. The Hamiltonian of this system is (in angular frequency units)

$$H = \sum_{i=1}^3 \omega_i I_z^i + 2\pi \sum_{i<j}^3 J_{ij} I_z^i I_z^j, \quad (6)$$

where  $I_z^i$ 's are the local spin operators. The  $\omega_i$  are the Larmor frequencies of the individual qubits. Relevant are the frequency differences  $\omega_1 - \omega_2 \approx 12.02$  kHz and  $\omega_2 - \omega_3 \approx 17.33$  kHz, and the coupling constants  $J_{12} = 64.2$ Hz,  $J_{13} = 51.3$ Hz, and  $J_{23} = -129.0$ Hz.

The system was first prepared in a pseudopure state (PPS)  $\rho_{000} = \epsilon(|000\rangle\langle 000| - \frac{1}{8}\mathbf{1})$ , where  $\epsilon \approx 10^{-5}$  describes the thermal polarization of the system. For this initial state preparation, we used spatial averaging [11] by the pulse sequence [12] shown in the first line of Fig. 3.

From the input state  $|000\rangle$ , we prepare the maximally entangled Bell state of qubits 2 and 3 with a Hadamard and a CNOT gate. The ancilla qubit 1 is then put into a superposition state by another Hadamard gate. The actual trajectories are implemented by rotating qubit 2, conditioned on the state of the ancilla qubit. This part of the pulse sequence is represented in the second and third line of Fig. 3. The actual rotation operations, which are implemented by the gray and hatched pulses, occur only on the second qubit, while the  $\pi$  rotations are applied for refocusing the coupling to qubit 3 while retaining the coupling with qubit 1.

In order to improve the fidelity of these operations, we implemented the pulses as robust strongly modulating pulses (SMP) [13, 14, 15]. We maximized the gate fidelity of the individual propagators for a suitable range of radio frequency field strengths. The theoretical fidelities over the relevant range of experimental parameters exceeded 0.995 for the individual gates, and the resulting pulse durations ranged from 200 to 500  $\mu\text{s}$ .

The algorithm requires the measurement of  $\langle \sigma_x^1 \rangle$ , the x-component of the ancilla qubit. In an NMR experiment, this corresponds to the first point of the free induction decay (FID) In practice, better results are obtained by

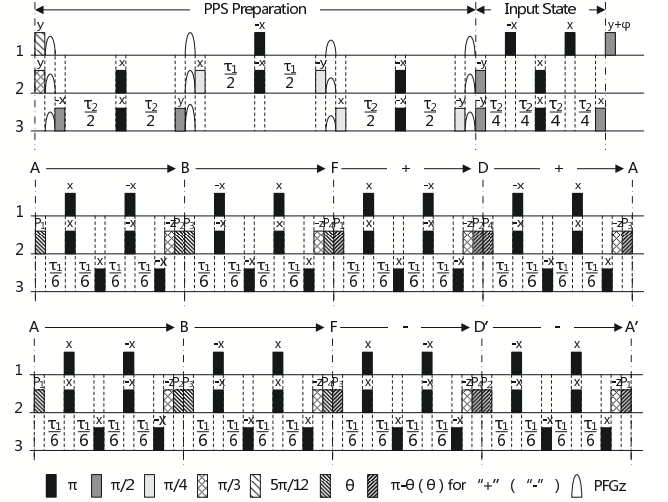


FIG. 3: Sequence of radio-frequency and field gradient pulses used for the preparation of the initial state (first line) and to drive the system through the different trajectories. The second line shows the sequence for the “+” trajectory, the third line for the “-”. The parameters are delays  $\tau_1 = 1/2J_{12}$  and  $\tau_2 = 1/2J_{23}$ , flip angle  $\theta = \arccos(1/\sqrt{3})$ , and phases  $P_1 = 3\pi/4$ ,  $P_2 = 7\pi/4$ ,  $P_3 = 5\pi/4$ ,  $P_4 = \pi/4$ .

recording the complete FID, Fourier-transforming it and integrating the signal over the relevant frequency range.

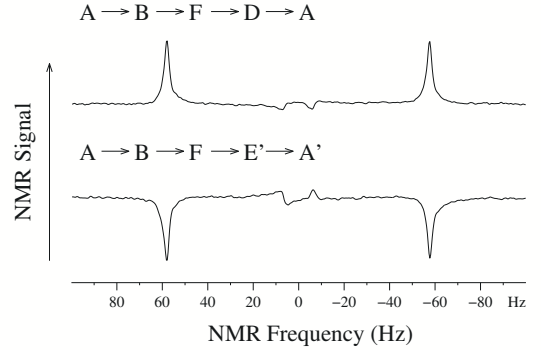


FIG. 4:  $^{19}\text{F}$  spectra of the ancilla qubit. The upper spectrum was obtained after the “+” trajectory was applied to qubit 2, the lower one after the “-” trajectory.

In the experimental spectra, shown in Fig. 4, the resonance line is split by the coupling to the second qubit. While the algorithm only requires the measurement of the integrated signal, the lineshapes and the relative amplitudes provide useful additional information about the quality of the measurement. Ideally, both resonance lines should have absorption lineshapes and the amplitudes should be equal. Obviously, the experimental data agree well with these predictions.

The upper spectrum was obtained after applying the “+” trajectory (red curve in Fig. 1). In this case, the

signal amplitude is positive, indicating that the trajectory did not change the phase of the quantum state. In the lower trace, we show the corresponding data after the system underwent the conditional “-” trajectory. In this case, the signal is inverted, as expected for a  $\pi$  phase change.

As an additional check that the observed sign change arises from a phase angle acquired during the trajectory, we measured a complete interferogram, by shifting the relative phase of the two states of the ancilla qubit and measuring the signal for each phase value.

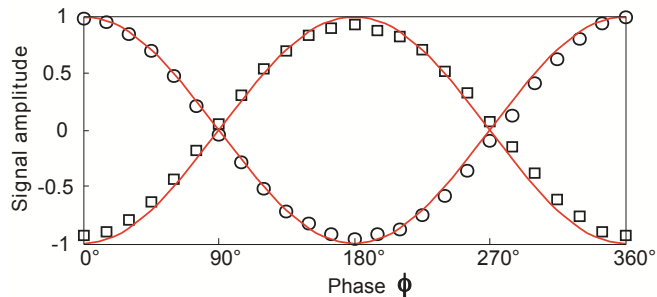


FIG. 5: (Color online) Experimental interference patterns. The squares represent the experimental data points for the “-” trajectory, the circles those of the “+” class. The lines represent the corresponding theoretical functions.

Figure 5 compares the experimentally observed signal amplitudes to the theoretical curve

$$\langle \sigma_x^1 \rangle = \cos(\varphi - \gamma_{\pm}).$$

$\varphi$  is the experimentally introduced phase shift, which corresponds to a delay in one arm of a Mach-Zehnder interferometer and  $\gamma_{\pm} = \{0, \pi\}$  is the phase change due to the circuit. The agreement between the theoretical and experimental data is quite satisfactory and clearly verifies the expected phase shift of  $\pi$  for the “-” trajectory.

When a quantum state undergoes a cyclic trajectory, it acquires a phase factor that includes a geometrical part [2, 3, 4, 5]. This geometrical phase is given by the total curvature of the surface enclosed by the circuit. A small variation of that circuit leads therefore, in general, to a small change of the geometrical phase.

The situation is different in the present case: small variations of the trajectory do not change the overall phase factor [8]. Instead, we only have two classes of trajectories: if the trajectory crosses the surface of the  $SO(3)$  sphere an even number of times (including 0), the total phase vanishes; if the number of crossings is odd, the state reverses its sign. The different behavior of these two classes of trajectories is directly related to the double connectedness of  $SO(3)$ , and the observed phase factor may therefore be called a topological phase. A related situation is that of conical intersections [16, 17], where the phase change does not depend on the area enclosed by the circuit, but only by the number of times it encircles the point of intersection. Possible extensions of this work include the investigation of multi-qubit systems for different degrees of entanglement and noncyclic evolutions. These results may be relevant for topological quantum computation [18, 19].

#### Acknowledgments

We acknowledge the support by National Natural Science Foundation of China, the CAS, Ministry of Education of PRC, and the National Fundamental Research Program. This work is also supported by the DFG under contract Su 192/19-1, and by the European Commission under contract No. 007065 (Marie Curie Fellowship).

*Note added.* After we finished the experiments, we became aware of a related optical experiment [20].

- 
- [1] F. Wilczek, Phys. Rev. Lett. **49**, 957 (1982).  
[2] S. Pancharatnam, Proc. Ind. Acad. Sci. **44**, 247 (1956).  
[3] M. Berry, Proc. Roy. Soc. London **A392**, 45 (1984).  
[4] Y. Aharonov and J. Anandan, Phys. Rev. Lett. **58**, 1593 (1987).  
[5] A. Bohm, A. Mostafazadeh, H. Koizumi, Q. Niu, and J. Zwanziger, *The Geometric Phase in Quantum Systems* (Heidelberg: Springer-Verlag, 2003).  
[6] P. Milman, Phys. Rev. A **73**, 062118 (2006).  
[7] P. Milman and R. Mosseri, Phys. Rev. Lett. **90**, 230403 (2003).  
[8] W. LiMing, Z. L. Tang, and C. J. Liao, Phys. Rev. A **69**, 064301 (2004).  
[9] D. Suter, K. T. Mueller, and A. Pines, Phys. Rev. Lett. **60**, 1218 (1988).  
[10] J. Du, P. Zou, M. Shi, L. C. Kwek, J.-W. Pan, C. H. Oh, A. Ekert, D. K. L. Oi, and M. Ericsson, Phys. Rev. Lett. **91**, 100403 (2003).  
[11] D. G. Cory, M. D. Price, and T. F. Havel, Physica D: Nonlinear Phenomena **120**, 82 (1998).  
[12] X. Peng, X. Zhu, X. Fang, M. Feng, X. Yang, M. Liu, and K. Gao, arXiv.org:quant-ph/0202010 (2002).  
[13] E. M. Fortunato, M. A. Pravia, N. Boulant, G. Teklemariam, T. F. Havel, and D. G. Cory, The Journal of Chemical Physics **116**, 7599 (2002).  
[14] M. A. Pravia, N. Boulant, J. Emerson, E. M. F. and Timothy F. Havel, R. Martinez, and D. G. Cory, The Journal of Chemical Physics **119**, 9993 (2003).  
[15] T. S. Mahesh and D. Suter, Phys. Rev. A **74**, 062312 (2006).  
[16] G. Herzberg and H. Longuet-Higgins, Discuss. Faraday Soc. **35**, 77 (1963).  
[17] C. A. Mead and D. G. Truhlar, J. Chem. Phys. **70**, 2284 (1979).

- [18] A. Y. Kitaev and L. Landau, *Annals of Physics* **303**, 2 (2003).
- [19] H. Bombin and M. A. Martin-Delgado, *Phys. Rev. Lett.* **98**, 160502 (2007).
- [20] C. Souza, J. Huguenin, P. Milman, and A. Houry, *arXiv:0704.0893v1* (2007).